JACS
JOURNAL OF THE AMERICAN CHEMICAL SOCIETY
Communication
pubs.acs.org/JACS

Conversion of Dinitrogen to Ammonia by FeN_3-Embedded Graphene

Xiao-Fei Li,*[,†] Qin-Kun Li,[†] Jin Cheng,[†] Lingling Liu,[†] Qing Yan,[†] Yingchao Wu,[†] Xiang-Hua Zhang,[†] Zhi-Yong Wang,[†] Qi Qiu,[†] and Yi Luo[‡]

[†]School of Optoelectronic Information, University of Electronic Science and Technology of China, Chengdu, Sichuan 610054, China
[‡]Hefei National Laboratory for Physical Sciences at the Microscale and Synergetic Innovation Center of Quantum Information and Quantum Physics, University of Science and Technology of China, Hefei, Anhui 230026, China

Supporting Information

ABSTRACT: Nitrogen fixation is one of the most important issues but a long-standing challenge in chemistry. Here, we propose FeN_3-embedded graphene as the catalyst for nitrogen fixation from first-principles calculations. Results show that in view of the chemical coordination, the FeN_3 center is highly spin-polarized with a localized magnetic moment substantially to promote N_2 adsorption and activate its inert N-N triple bond. The synergy between the graphene and FeN_3 equips the system with novel features for the catalytic conversion of the activated N_2 into NH_3 via a six-proton and six-electron process, following three possible reaction pathways at room temperature. Our findings provide a rational paradigm for catalytic nitrogen fixation that would be conducive to ammonia production.

Dinitrogen (N_2) is abundant in atmosphere, yet it can merely be utilized directly by a few organisms with endophytic diazotrophic bacteria and otherwise intermediately absorbed only after being converted to ammonia (NH_3) or nitride. Dinitrogen-fixation (N_2-fixation) thus is one of the most fascinating conversions in biochemistry.[1−6] Research has shown that biological N_2-fixation occurs under ambient conditions with the aid of nitrogenase enzymes and that the active sites are rich in Fe and S and can additionally contain Mo or V atoms,[6,7] but the detailed mechanism remains elusive.[8−10] In contrast, the Fe or Ru catalysts are analogously employed to break the inert triple bond of N_2 in the industrial Haber−Bosch process for N_2-fixation, but extreme reaction conditions are still commanded and only a very low percent of the consumed energy would be converted into NH_3.[11] Thus, it is essential to understand the underlying mechanisms of nitrogenases and design efficient catalysts for conversion of N_2 to NH_3 under mild conditions.[8,12]

Imitating the biological process, the state-of-the-art catalysts for N_2-fixation are mainly transition metal-dinitrogen (TM-N_2) complexes.[2,4,7,13−18] For example, Shima et al.[19] propose a $[(C_5Me_4SiMe_3)Ti]_3$-N_2 as the platform for N_2-fixation, whereas Yandulov et al.[13] propose a [HIPTN$_3$N]Mo-N_2 center, Arashiba et al.[14] employ two Mo-N_2 complexes bearing PNP [Mo-$(N_2)_2$(PNP)]$_2$(μ-N_2), and Banerjee et al.[20] explore the FeMoS-chalcogels as catalysts for N_2-fixation under ambient conditions. These systems generally adopt Mo-N_2 complexes facilitating the conversion process.[8,9] However, spectroscopic studies implicate that iron is the essential TM atom for N_2 binding in FeMo-cofactor of nitrogenases,[21] and Fe has received the most attention because of its robustness and low cost.[18,22] Recently, Anderson et al.[4,7] report the (TPB)Fe-N_2, Rodriguez et al.[22] explore a molecular iron-potassium system supported Fe-N_2, and Peters et al.[2,15] propose the [Si(o-$C_6H_4PR_2)_3$]Fe-N_2 for N_2-fixation, respectively. Their results suggest that Fe-N_2-mediated N_2-fixation is really accessible.[16,18] Aiming to guarantee that the TM sites are highly active and stable during the catalytic process, metal hydride clusters or organic ligands were used to confine the TM atoms. Yet the precise intermediates are pretty difficult to identify due to the complicated construction of the proposed models, rendering the mechanistic details obscure.[10,22,23]

Graphene has a simple two-dimensional structure but novel properties. Very recently, it was reported that N-doped graphene (N-graphene) affords an excellent ability for catalyzing the oxygen reduction reaction (ORR).[24,25] Here, we propose N-graphene supported Fe-N_2 complex to catalyze N_2-fixation under ambient conditions from first-principles calculations. We find that the high-spin polarization of the Fe site is responsible for the superior N_2 activity and the subsequent N_2-fixation process.

All the calculations were carried out by means of spin-resolved density functional theory including vdW corrections as implemented in VASP-5.3,[26] using the projector augmented wave pseudopotential for the core electrons, a 500 eV cutoff energy for the plane-wave basis set for the valence electrons, and the revised Perdew−Burke−Ernzerhof generalized gradient approximation for the exchange−correlation potential.

We first checked the possibility to embed an Fe atom in the single and double vacancies (SV, DV) formed in graphene by multinitrogen-atom doping (N_x-graphene, x = 3,4). We find that the binding energies of the resultant FeN_3- and FeN_4-graphene are −5.13 and −7.35 eV with the cohesive energy of atomic Fe and are −1.90 and −4.12 eV with bulk Fe, respectively, suggesting that an Fe atom would be tightly anchored in SV or DV, but the latter binds stronger. According to the reports that the configuration of N-graphene is substantially governed by the type of vacancies in graphene,[27,28] although only FeN_4 is identified currently,[29,30] FeN_3 can also be formed in graphene under proper conditions based on our calculations, since N_3-graphene has already been synthesized in experiments recently and proposed for other applications.[31−34]

Received: May 9, 2016
Published: July 6, 2016

DOI: 10.1021/jacs.6b04778
J. Am. Chem. Soc. 2016, 138, 8706−8709

It is reported that when an Fe atom is embedded directly in SV of graphene, the system is not magnetic.[35] Our calculations show that either the Fe atom embedding in SV of N_3-graphene (as shown in Figure 1a) or DV of N_4-graphene, the system is always

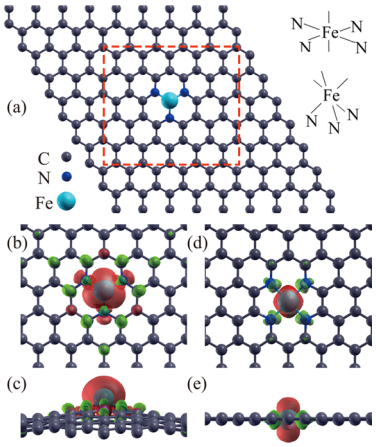

Figure 1. Optimized structure of (a) FeN_3-graphene and its isosurface of the spin-resolved density pictures: (b) top and (c) side views. As comparison, the isosurface of FeN_4-graphene is also shown in (d) top and (e) side views. The isovalue is set to be 0.002 $eÅ^{-2}$, and the insets are the chemical coordination of the Fe at the FeN_3 and FeN_4 centers, respectively.

magnetic. The energy differences between the spin-polarized state and nonpolarized state of the disparate structures are about −1.20 and −1.78 eV, respectively, suggesting the stability of the spin-polarized ground state at room temperature. The spin moments of the FeN_3-graphene and FeN_4-graphene are 3.16 and 2.00 μ_B, respectively. The value of the FeN_4-graphene coincides well with the previous work,[31] while, the spin moment of the Fe at SV increases drastically from 0 to 3.16 μ_B after N-doping. Replacing three C atoms with N atoms, the system obtains an odd number of electrons and half-occupied states, inducing the spin-polarized ground state.[36]

To further clarify such behavior, we presented the top and side views of the spin-resolved density of FeN_3-graphene in Figure 1b,c and that of FeN_4-graphene in Figure 1d,e, respectively. One can see that the FeN_3-graphene has a nonplanar geometry in C_{3v} symmetry, the Fe atom stands out of graphene plane, and the charge clouds distribute at the vicinity of Fe, indicating that the main part of spin moment comes from Fe atom. According to the geometry, we drew the chemical coordination of Fe in the FeN_3 in the inset of Figure 1. One can see immediately that at least 3 μ_B of the spin moment (95%) comes from Fe atom. As for FeN_4-graphene, the Fe atom is totally incorporated into graphene layer due to coordination structure that modifies the residual chemical coordination number of Fe dramatically (see inset for details), resulting in a smaller spin moment (2.00 μ_B) which is divided into two segments and distributed on the Fe atom in mirror symmetry. Spin moment is proved to be vital for the catalysts to N_2-activation.[29,31] Thus, the FeN_3-graphene is of comparative interest, since it has a rather larger and more centralized spin moment and the bulged Fe atom is exposed in apical position above the graphene layer, which indicates the superiority for N_2 adsorption.

Our calculations show that a N_2 indeed would be well captured by the FeN_3-graphene. In the formed Fe-N_2 complex, the N_2 can be either standing-on (α) or lying-on (β) the Fe site as shown in Figure 2a,b, respectively. The adsorption energies of Fe-αN_2 and Fe-βN_2 are about −1.25 and −1.26 eV, respectively, suggesting

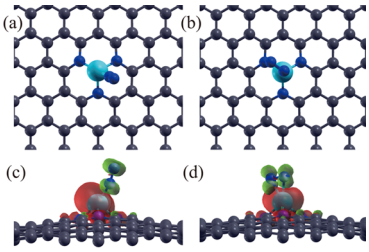

Figure 2. Optimized structures of the systems formed by adsorbing a N_2 on the FeN_3-graphene in (a) standing-on and (b) lying-on fashions, and the spin-resolved density pictures of the (c) standing-on and (d) lying-on geometry, respectively.

their good and equal stability at room temperature. The N−N bond lengths in Fe-α N_2 and Fe-βN_2 are about 1.15 and 1.18 Å, while the calculated lengths of the N≡N triple and N═N double bonds in the free N_2 and N_2H_2 are about 1.12 and 1.24 Å, respectively. Implicitly, the N−N bond orders in Fe-αN_2 and Fe-βN_2 are respectively about 2.75 and 2.5, indicating the great activating ability of the FeN_3 center to N_2 by adsorption.

Noteworthy is that the spin moments of Fe-αN_2 and Fe-βN_2 complexes are 3.27 and 3.13 μ_B, and the energy differences between the spin-polarized and nonpolarized states are about −0.87 and −1.47 eV, respectively. This means that even after N_2 adsorption, the system retains a heavily spin-polarized ground state even at room temperature. We figured out the spin-resolved density of Fe-αN_2 and Fe-βN_2 in Figure 2c,d, respectively. Clearly, the charge clouds are localized and distributed on both the adsorbed N_2 and Fe-N_3 center, suggesting the N_2 is indeed activated. Hence, the subsequent process to convert the activated N_2 to NH_3 by hydrogenation is highly desired.

We have similarly carried out the possibility to activate N_2 by FeN_4-graphene, whereas the N_2 can merely be adsorbed in standing-on fashion with a small adsorption energy (0.28 eV), indicating that the N_2 can not be well captured by the FeN_4 center. Noticing that the spin moment of FeN_4 center is divided into two segments, making each side of the graphene deficient, while the unusable strong N−N triple bond causes N_2, rather "uphill", to be polarized. Thus, although TMN_4-graphene systems maintain some interesting properties[29,31] and have been proposed for catalyzing oxidation of benzene and ORRs,[30,37] FeN_4-graphene performs inadequately as the catalyst for N_2-activation.

To obtain details of the conversion of the activated N_2 to NH_3 on FeN_3-graphene, we calculated the key reaction steps and products during the conversion process and canvassed the distal,[38] alternating,[7,11,39] and enzymatic[23] mechanisms. Three feasible reaction pathways, plus a hybrid path, were revealed, and their schematic diagrams are illustrated in Figure 3. Each pathway is a 6-proton and 6-electron process, which can be divided into 7 steps as the step of the NH_3-release and N_2-adsorption is included, but the sequence depends. One can see in the distal pathway that the consecutive protonation occurs first at the distal N and then at the proximal N. The successive 1−4 steps result in the full scission of the N−N bond and release of an NH_3, while the second NH_3 is released in the subsequent 5−7 steps and the Fe-N_2 is regenerated, indicating the feasibility of the cycle of adsorbing N_2 and releasing NH_3. For both the alternating and enzymatic pathways, the protonation alternates between the two

DOI: 10.1021/jacs.6b04778
J. Am. Chem. Soc. 2016, 138, 8706−8709

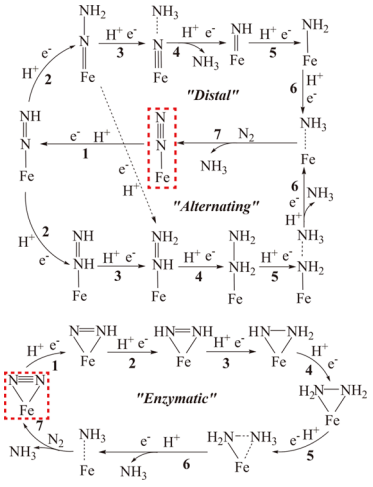

Figure 3. Schematic depiction of the three reaction pathways for conversion of N_2 to NH_3 catalyzed by FeN_3-graphene; the dotted arrow represents the hybrid path that transforms from distal to alternating pathway. For clarity, the N_3-graphene is not shown.

N atoms, making the first NH_3 release at the sixth step. Calculations also reveal a hybrid path which shifts from the distal to alternating pathway, as shown with the dotted arrow in Figure 3, implying the complex nature of N_2-fixation.

We carried out the reaction energy at each step of each pathway. The energies of proton and electron ($E(H^+)$, $E(e^-)$) were calculated by employing the model of Lutidinium ($[2,6\text{-LutH}]^+$) and $[CoCp^*_2]$, as suggested in the refs 23 and 40. The obtained $E(H^+)$ and $E(e^-)$ are about −10.24 and −4.51 eV, respectively, coinciding well with the previous reports. The reaction energy was calculated, the first step in distal pathway, for example, using the equation: $\Delta E = E(\text{Fe-N=NH}) - [E(\text{Fe-N}\equiv\text{N}) + E(H^+) + E(e^-)]$. Other steps were calculated in a similar way accordingly. The data are summarized in Table S3, and the reaction energies are plotted in Figure 4a.

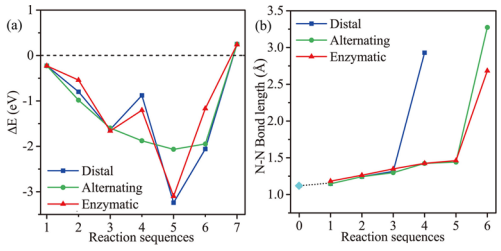

Figure 4. Reaction energy (a) and the N−N bond length (b) in Fe-N_2 complex along the three pathways. The dots in (b) illustrate the N−N bond length from free N_2 to N≡N cleavage and the first dot in the reaction sequence 0 represents the free N_2.

One can see clearly that almost each step releases energy except for the last step, desorption of the second NH_3. We know that the reaction, $N_2 + H_2 \rightarrow NH_3$, occurring in the industrial Haber−Bosch process, is actually exothermic but is hard to occur due to the difficulty of N_2-activation. Once it is activated, the activation barrier for the subsequent steps is usually relatively low and surmountable at room temperature.[6] In our Fe-N_2 complex, the first step of the hydrogenation in each pathway is always exothermic, suggesting that the N_2 is sufficiently activated and the energy barrier for N-N bond cleavage is greatly lowered by FeN_3 center at the adsorption step. The reaction energy of the Fe = N-NH_2 to Fe-NH-NH_2 is −1.92 eV, suggesting the feasibility of the hybrid path.

Desorption process is normally endothermic. We found that the release of the first NH_3 in distal, alternating, and enzymatic pathways needs to absorb energy of 0.03, 0.11, and 0.89 eV, respectively, suggesting that the split of N−N bond can energetically occur via either the distal or alternating pathway, but it might be largely hindered in the enzymatic pathway at room temperature. On the other hand, the released energy at the corresponding hydrogenation step is large enough to reduce this intermediate and release the first NH_3 exothermically as shown in Figure 4a. Thus, the FeN_3 center can take each of the three pathways to split the N-N bond.

After the N−N bond split, the reaction energies of the remaining hydrogenation steps are still negative, until the last step to release the second NH_3, which is endothermic by absorbing the same energy of 0.25 eV in each pathway. This small energy requirement indicates that it is energetically allowed to occur at room temperature.

We also considered the release of the intermediate of hydrazine (N_2H_4). The release of N_2H_4 requires the absorption of energy, ∼1.37 and 1.11 eV, respectively, in alternating and enzymatic pathways, implying this process would not occur at room temperature. Hence, FeN_3-graphene is unquestionably eligible to activate N_2 and convert it into NH_3 at room temperature.

We recorded the N−N bond lengths in each step of the pathways and plotted them in Figure 4b. Step 0 represents free N_2. One can see that the N−N bond is first stretched by the adsorption and then elongated by the hydrogenation stepwise, until it breaks at the fourth or sixth step. The nearly linear variation of N−N bond indicates that the stretching effect of adsorption is comparable to that of the hydrogenation, implying the considerable ability of the Fe-N_3 to activate N_2.

To gain further insights into the catalytic effect of the FeN_3-graphene on the N_2-fixation, we performed charge population analysis. Each intermediate was divided into three moieties: graphene (moiety1), FeN_3 (moiety2), and the bounded N, H atoms (moiety3), as illustrated in Figure 5a. The charge variation, defined as the Mulliken atomic charge difference of each moiety in the present step from that of the previous step, for each intermediate along the distal, alternating, and enzymatic

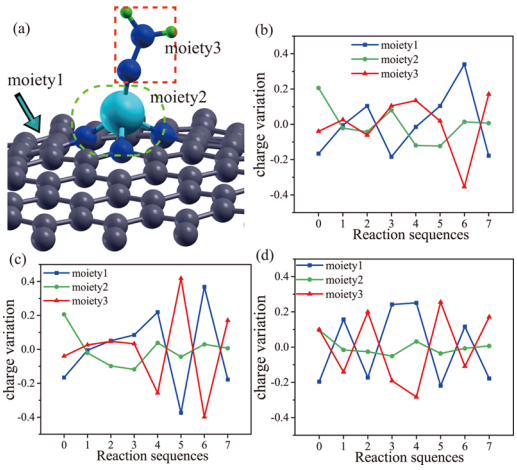

Figure 5. Three moieties of the Fe-N=NH_2 intermediate, for example, and the charge variation of the three moieties along the distal (b), alternating (c) and enzymatic (d) pathways, respectively.

DOI: 10.1021/jacs.6b04778
J. Am. Chem. Soc. 2016, 138, 8706−8709

pathways is plotted in Figure 5b–d, respectively. The charge variation at step 0 represents the transferred charges during N_2 adsorption. For the standing-on configuration, one can see in Figure 5b,c that the FeN_3 gains ~0.21 electrons from graphene. While for the lying-on configuration, both the FeN_3 and N_2 moieties gain about 0.1 electrons from graphene (see Figure 5d). FeN_3 is involved in adsorption process as expected, and the graphene acts as an electron reservoir ascribing to the high charge density.

For the subsequent hydrogenation process, FeN_3 may be involved in the reaction or only serve as the transmitter to transfer electrons. One can see that the FeN_3 and the moiety3 gain almost the same number of electrons from graphene at the third step of the distal pathway and that FeN_3 contributes electrons to both graphene and moiety3 at the third step of the alternating pathway, but has only a very small charge fluctuation along the enzymatic pathway. Thus, the role of the FeN_3-graphene can be identified: The graphene is electron reservoir, the FeN_3 is the active site for N_2-fixation and the transmitter for electron transfer, and the collaboration between them contributes to the system to be a novel catalyst for N_2-fixation.

In conclusion, by performing first-principles calculations, we have proposed a new catalyst for activating N_2 and converting it into NH_3 at room temperature. The high-spin polarization of the FeN_3 center is responsible for the superior N_2 fixation activity. Since the TM atoms of Sc, V, and Mn, embedded at the defect of graphene, result in a high-spin polarization,[35] it is expected that, although the Fe is the only essential TM atom in nitrogenases, these TM atoms are also the possible active-site for N_2-fixation.

■ ASSOCIATED CONTENT

Supporting Information

The Supporting Information is available free of charge on the ACS Publications website at DOI: 10.1021/jacs.6b04778.

Calculational details and data (PDF)

■ AUTHOR INFORMATION

Corresponding Author

*xf.li@uestc.edu.cn

Notes

The authors declare no competing financial interest.

■ ACKNOWLEDGMENTS

We acknowledge the support from the National Natural Science Foundation of China (21421063) and Strategic Priority Research Program of Chinese Academy of Sciences (XDB01020200).

■ REFERENCES

(1) Karl, D.; Letelier, R.; Tupas, L.; Dore, J.; Christian, J.; Hebel, D. *Nature* **1997**, *388*, 533.
(2) Rittle, J.; Peters, J. C. *J. Am. Chem. Soc.* **2016**, *138*, 4243.
(3) Galloway, J. N.; Townsend, A. R.; Erisman, J. W.; Bekunda, M.; Cai, Z.; Freney, J. R.; Martinelli, L. A.; Seitzinger, S. P.; Sutton, M. A. *Science* **2008**, *320*, 889.
(4) Anderson, J. S.; Moret, M.-E.; Peters, J. C. *J. Am. Chem. Soc.* **2013**, *135*, 534.
(5) Canfield, D. E.; Glazer, A. N.; Falkowski, P. G. *Science* **2010**, *330*, 192.
(6) Hoffman, B. M.; Lukoyanov, D.; Yang, Z.-Y.; Dean, D. R.; Seefeldt, L. C. *Chem. Rev.* **2014**, *114*, 4041.
(7) Anderson, J. S.; Rittle, J.; Peters, J. C. *Nature* **2013**, *501*, 84.
(8) Schrock, R. R. *Angew. Chem., Int. Ed.* **2008**, *47*, 5512.
(9) Stüeken, E. E.; Buick, R.; Guy, B. M.; Koehler, M. C. *Nature* **2015**, *520*, 666.
(10) Howard, J. B.; Rees, D. C. *Proc. Natl. Acad. Sci. U. S. A.* **2006**, *103*, 17088.
(11) van der Ham, C. J.; Koper, M. T.; Hetterscheid, D. G. *Chem. Soc. Rev.* **2014**, *43*, 5183.
(12) Tanabe, Y.; Nishibayashi, Y. *Coord. Chem. Rev.* **2013**, *257*, 2551.
(13) Yandulov, D. V.; Schrock, R. R. *Science* **2003**, *301*, 76.
(14) Arashiba, K.; Miyake, Y.; Nishibayashi, Y. *Nat. Chem.* **2011**, *3*, 120.
(15) Lee, Y.; Mankad, N. P.; Peters, J. C. *Nat. Chem.* **2010**, *2*, 558.
(16) Creutz, S. E.; Peters, J. C. *J. Am. Chem. Soc.* **2014**, *136*, 1105.
(17) MacLeod, K. C.; Vinyard, D. J.; Holland, P. L. *J. Am. Chem. Soc.* **2014**, *136*, 10226.
(18) Crossland, J. L.; Tyler, D. R. *Coord. Chem. Rev.* **2010**, *254*, 1883.
(19) Shima, T.; Hu, S.; Luo, G.; Kang, X.; Luo, Y.; Hou, Z. *Science* **2013**, *340*, 1549.
(20) Banerjee, A.; Yuhas, B. D.; Margulies, E. A.; Zhang, Y.; Shim, Y.; Wasielewski, M. R.; Kanatzidis, M. G. *J. Am. Chem. Soc.* **2015**, *137*, 2030.
(21) Hoffman, B. M.; Dean, D. R.; Seefeldt, L. C. *Acc. Chem. Res.* **2009**, *42*, 609.
(22) Rodriguez, M. M.; Bill, E.; Brennessel, W. W.; Holland, P. L. *Science* **2011**, *334*, 780.
(23) Le, Y.-Q.; Gu, J.; Tian, W. Q. *Chem. Commun.* **2014**, *50*, 13319.
(24) Li, J.; Zhang, Y.; Zhang, X.; Han, J.; Wang, Y.; Gu, L.; Zhang, Z.; Wang, X.; Jian, J.; Xu, P.; Song, B. *ACS Appl. Mater. Interfaces* **2015**, *7*, 19626.
(25) Guo, D.; Shibuya, R.; Akiba, C.; Saji, S.; Kondo, T.; Nakamura, J. *Science* **2016**, *351*, 361.
(26) Kresse, G.; Hafner, J. *Phys. Rev. B: Condens. Matter Mater. Phys.* **1994**, *49*, 14251.
(27) Wang, B.; Tsetseris, L.; Pantelides, S. T. *J. Mater. Chem. A* **2013**, *1*, 14927.
(28) Li, X.-F.; Lian, K.-Y.; Liu, L.; Wu, Y.; Qiu, Q.; Jiang, J.; Deng, M.; Luo, Y. *Sci. Rep.* **2016**, *6*, 23495.
(29) Lin, Y.-C.; Teng, P.-Y.; Chiu, P.-W.; Suenaga, K. *Phys. Rev. Lett.* **2015**, *115*, 206803.
(30) Deng, D.; Chen, X.; Yu, L.; Wu, X.; Liu, Q.; Liu, Y.; Yang, H.; Tian, H.; Hu, Y.; Du, P.; Si, R.; Wang, J.; Cui, X.; Li, H.; Xiao, J.; Xu, T.; Deng, J.; Yang, F.; Duchesne, P. N.; Zhang, P.; Zhou, J.; Sun, L.; Li, J.; Pan, X.; Bao, X. *Sci. Adv.* **2015**, *1*, e1500462.
(31) Kattel, S.; Atanassov, P.; Kiefer, B. *J. Phys. Chem. C* **2012**, *116*, 8161.
(32) Tison, Y.; Lagoute, J.; Repain, V.; Chacon, C.; Girard, Y.; Rousset, S.; Joucken, F.; Sharma, D.; Henrard, L.; Amara, H.; Ghedjatti, A.; Ducastelle, F. *ACS Nano* **2015**, *9*, 670.
(33) Joucken, F.; Tison, Y.; Lagoute, J.; Dumont, J.; Cabosart, D.; Zheng, B.; Repain, V.; Chacon, C.; Girard, Y.; Botello-Mendez, A. R. *Phys. Rev. B: Condens. Matter Mater. Phys.* **2012**, *85*, 161408.
(34) Usachov, D.; Vilkov, O.; Grĺzneis, A.; Haberer, D.; Fedorov, A.; Adamchuk, V. K.; Preobrajenski, A. B.; Dudin, P.; Barinov, A.; Oehzelt, M.; Laubschat, C.; Vyalikh, D. V. *Nano Lett.* **2011**, *11*, 5401.
(35) Krasheninnikov, A. V.; Lehtinen, P. O.; Foster, A. S.; Pyykkö, P.; Nieminen, R. M. *Phys. Rev. Lett.* **2009**, *102*, 126807.
(36) Li, X.-F.; Lian, K.-Y.; Qiu, Q.; Luo, Y. *Nanoscale* **2015**, *7*, 4156.
(37) Kattel, S.; Wang, G. *J. Phys. Chem. Lett.* **2014**, *5*, 452.
(38) Chatt, J.; Dilworth, J. R.; Richards, R. L. *Chem. Rev.* **1978**, *78*, 589.
(39) Anderson, J. S.; Cutsail, G. E., III; Rittle, J.; Connor, B. A.; Gunderson, W. A.; Zhang, L.; Hoffman, B. M.; Peters, J. C. *J. Am. Chem. Soc.* **2015**, *137*, 7803.
(40) Schenk, S.; Le Guennic, B.; Kirchner, B.; Reiher, M. *Inorg. Chem.* **2008**, *47*, 3634.

DOI: 10.1021/jacs.6b04778
J. Am. Chem. Soc. 2016, 138, 8706–8709